35th Annual International Conference of the IEEE EMBS
Osaka, Japan, 3 - 7 July, 2013

Atlas-based segmentation of white matter structures from DTI using tensor invariants and orientation

Rodrigo de Luis-García, Gonzalo Vegas Sánchez-Ferrero, Santiago Aja Fernández and Carlos Alberola-López

Abstract— **This paper presents a novel method for the segmentation of anatomical structures in the white matter from DTI (*Diffusion Tensor Imaging*) data. Our approach is based on: (a) the use of a DTI white matter atlas to guide the segmentation process, (b) the use of tensor invariants and the orientation information of the tensor as features, and (c) a statistical modeling of the data with a level set implementation. This formulation allows for controlling the relative importance of the different properties of the diffusion tensor and uses the anatomical information of the atlas to constrain the segmentation. The method has been applied to the segmentation of DTI volumes, and results show it constitutes a valid alternative to other approaches such as VBM or TBSS for white matter analysis.**

I. Introduction

DTI analysis of brain structures has shown to be relevant in a number of neurological pathologies, such as brain ischemia, epilepsy, schizophrenia or Alzheimer's disease, among others [19], [16], [8], [17]. Thus, the automatic segmentation of these structures from DTI has spurred significant research effort recently.

However, many of the methods proposed in the literature ([9], [2], [22], [14], [4], [3]) present several drawbacks. First, many require the manual identification of a region of interest or starting seeds for the segmentation to be performed, or some other kind of user interaction. Second, accuracy concerns arise in situations where diffusion tensors are similar to adjacent but distinct white matter structures under the chosen tensor metric.

This paper addresses the problem of creating an automatic segmentation approach which is capable of accurately segmenting anatomical structures within the white matter. Two novel elements are designed to overcome the drawbacks mentioned before.

The first element is the use of a DTI atlas of human white matter [11], which is nonlinearly registered to the volume under study. Atlas-based segmentation is carried out by means of the registration of an atlas, which has been manually segmented, onto the image under study. The manual segmentation is then transformed into the space of the image under study through the obtained transformation. If the registration is completely accurate, then the segmentation result should be correct. However, obtaining a totally accurate registration is unrealistic, especially when dealing with DTI data. Therefore, the segmentation method proposed does not rely entirely on the atlas registration, but uses the atlas to guide the segmentation in two ways: first, to provide an initial segmenting surface for the segmentation process that will be close to the correct segmentation, thus avoiding local minima; second, to create a spatial prior that favors solutions close to the registered segmented object during the segmentation process. Using both techniques, the segmentation is guided by the image data but constrained, to a certain extent, by the information available through the atlas.

As for the second element, we employ tensor invariants, together with the orientation of the tensor, as features to drive the segmentation. Most recent approaches in the literature employ intrinsic tensor dissimilarity measures such as the Kullback-Leibler distance [21], the information geodesic distance [9] or the Log-Euclidean metric [1]. Even though they are compact and mathematically well founded, intrinsic tensor dissimilarity measures suffer from a major drawback: the influence of the different tensor properties in the distance cannot be controlled. For the segmentation of anatomical structures in the white matter, the tensor shape (and its different attributes) and its orientation are not always equally relevant. Tensors belonging to the corpus callosum and the cingulum, for instance, have similar shape but completely different orientations. Thus, adapting the segmentation process to the needs of each case can improve the accuracy and robustness of the results.

Results will be shown that demonstrate that the proposed approach is capable of accurately segmenting different structures of the white matter, such as the corpus callosum, the corona radiata, the cingulum or the external capsule, and how the proposed contributions help improve the accuracy and robustness of the segmentation.

II. Segmentation Method

Figure 1 shows a general diagram of the proposed segmentation pipeline. As can be seen, three main elements constitute the kernel of the segmentation: the white matter atlas registration, the use of a spatial prior and the representation of the tensor information by means of the tensor invariants and orientation. These elements are next studied in detail.

A. White Matter Atlas Registration

In this paper, we employed the so-called JHU MNI SS atlas, a single-subject atlas (a.k.a. *New Eve*) with a comprehensive white matter parcellation developed at Johns Hopkins University [20], [11].

The authors are with the Laboratory of Image Processing, University of Valladolid, Spain rodlui@tel.uva.es, gvegsan@lpi.tel.uva.es, sanaja@tel.uva.es, caralb@tel.uva.es

978-1-4577-0216-7/13/$26.00 ©2013 IEEE

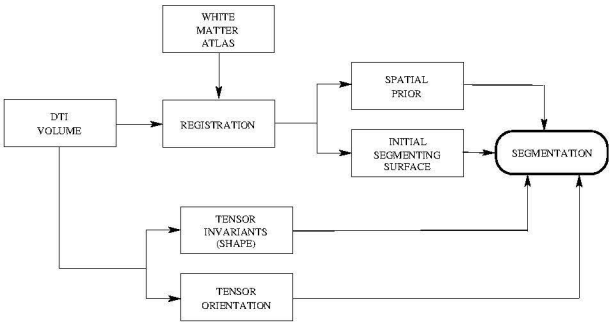

Fig. 1. General pipeline of the segmentation method proposed in this paper.

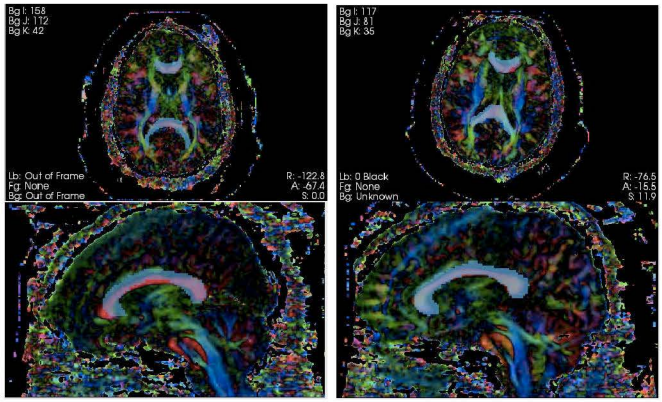

Fig. 2. Axial and sagittal views of the registered labelmap corresponding to the corpus callosum for two different DTI volumes. The labelmap is colored in light blue with a decreased opacity, so that the corpus callosum (in red because of the predominant tensor orientation) can be seen behind.

From the DTI data, FA scalar volumes were created both for the atlas and the volume under study. This volume is then registered to the atlas, using an affine registration algorithm using *flirt* utility from the FSL library of analysis tools [7], [18], and the inverse of the obtained transformation is applied to the atlas labelmap to generate the initial surface and spatial prior. Several methods for the registration of DTI have been reported in the literature [15], [12]. However, an affine registration from scalar FA volumes derived from the tensor data is preferred in this case, since it is a simpler approach and the registered labelmap is not expected to constitute an accurate segmentation of the structures of interest. As can be seen in Figure 2, only an approximate surface is obtained that must be refined through the segmentation process.

B. Geodesic Active Regions with Spatial Prior

In the proposed segmentation method, prior spatial information is available from the previous registration step which can guide the segmentation process. The registered labelmap of the segmented object gives an approximate segmentation, which however needs to be refined based on the image information. We show in Figure 3 a scheme of such a labelmap, which can be interpreted as the probability of pixel $\mathbf{x}$ to belong to the segmenting object i. The labelmap

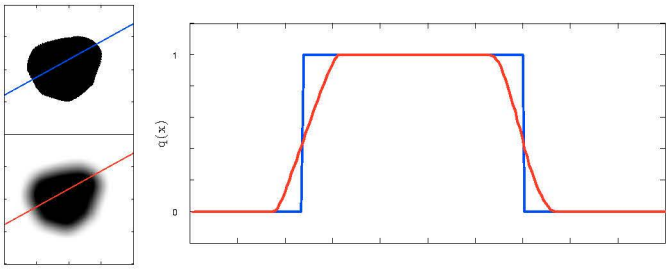

Fig. 3. Schematic labelmap (top left); Gaussian smoothed labelmap (bottom left); 1D cross-sections of the labelmap (blue) and its smoothed version (red), $q(\mathbf{x})$.

provides a binary probability, but it can be smoothed to account for a higher level of uncertainty near the boundaries of the segmented object. This smoothed labelmap is denoted by $q_i(\mathbf{x})$ and will be employed as a spatial prior throughout this work.

Using the *Geodesic Active Regions* (GAR) model [13] as a basis, the segmentation is formulated as the minimization of an energy functional that is equivalent to the maximization of the *a posteriori* frame partition. In order to perform the segmentation, the energy functional must be minimized with respect to the statistical parameters and to the segmenting surface, represented by means of the level set function $\phi(\mathbf{x})$. This is done following the two-step Expectation-Maximization technique[5]. For a fixed level set, the statistical parameters are updated with their ML estimators. Next, the segmenting surface is evolved following the level set equation:

$$\begin{aligned}\frac{\partial\phi}{\partial t}(\mathbf{x}) &= \delta(\phi)\left[\nu\nabla\cdot\left(\frac{\nabla\phi}{|\nabla\phi|}\right) - \log\left(\frac{p(\mathbf{v}(\mathbf{x})|\boldsymbol{\Theta_1})}{p(\mathbf{v}(\mathbf{x})|\boldsymbol{\Theta_2})}\right)\right. \\ &\quad \left. - \log\left(\frac{q_1(\mathbf{x})}{q_2(\mathbf{x})}\right)\right] \qquad (1)\end{aligned}$$

where $\delta(\phi)$ is the Dirac function. The image I is represented by the feature vector $\mathbf{v}(\mathbf{x})$, whose distribution over each region i is parameterized by $\boldsymbol{\Theta}_\mathbf{i}$. The last term within brackets does not appear in the original GAR formulation, and accounts for the influence of the shape prior introduced in this paper.

C. Tensor Invariants and Orientation

Instead of considering the tensor as a whole through the use of intrinsic tensor distances, we propose to treat the shape and the orientation of the tensor independently. In order to do so, let us first consider, for each point $\mathbf{x}$, the feature vector $\mathbf{K}(\mathbf{x})$ consisting of the three tensor invariants proposed in [6], $\mathbf{K} = [K_1\ K_2\ K_3]^T$, where $K_1 = \text{trace}(\mathbf{T})$; $K_2 = |\text{dev}(\mathbf{T})|$ and $K_3 = 3\sqrt{6}\det\left(\frac{\text{dev}(\mathbf{T})}{|\text{dev}(\mathbf{T})|}\right)$. $\text{dev}(\mathbf{T})$ is the deviatoric part of tensor $\mathbf{T}$. These three invariants, which are orthogonal, completely describe the tensor shape. K_1 represents the tensor size, while K_2 and K_3 describe the amount of anisotropy and the tensor mode, respectively.

In order to unambiguously represent the orientation of the main eigenvector $\mathbf{e}_1$ of the diffusion tensor, we compute

Anatomical Structure	α	β	ν
Corpus Callosum	0.2	0.25	1
Cingulum	0.3	1	0.2
Corona Radiata	0.3	0.25	1
Inf. Longitudinal Fasciculi	0.3	0.5	1

TABLE I

SEGMENTATION PARAMETERS FOR DIFFERENT STRUCTURES.

the outer product $\mathbf{U} = \mathbf{e}_1\mathbf{e}_1^T$, and take its six independent components $u_i (1 \leq i \leq 6)$.

Putting together the invariants and the orientation, the PDF of the feature vector that represents the tensor information can be expressed as:

$$p(\mathbf{v}|\mathbf{\Theta_i}) = \left[\prod_{j=1}^{3} p(K_j|\mathbf{\Theta_{K_j,i}})\right] \cdot p(\mathbf{u}|\mathbf{\Theta_{u,i}}) \qquad (2)$$

with $\mathbf{u} = [u_1\ u_2\ u_3\ u_4\ u_5\ u_6]^T$. $\mathbf{\Theta_{K_j,i}}$ and $\mathbf{\Theta_{u,i}}$ are the parameter sets describing the distributions of the tensor invariants and tensor orientation, respectively. $p(\mathbf{v}|\mathbf{\Theta_i})$ is then employed for the level set evolution equation, under a Gaussian assumption for the values of $K_j (1 \leq j \leq 3)$ and a multivariate Gaussian assumption for $\mathbf{u}$. The final level set evolution equation can be shown to be:

$$\frac{\partial\phi}{\partial t}(\mathbf{x}) = \delta(\phi)\left[\nu\nabla\cdot\left(\frac{\nabla\phi}{|\nabla\phi|}\right) - \alpha\sum_{j=1}^{3}\log\left(\frac{p(K_j(\mathbf{x})|\mathbf{\Theta}_{K_{j,1}})}{p(K_j(\mathbf{x})|\mathbf{\Theta}_{K_{j,1}})}\right)\right.$$
$$\left. - (1-\alpha)\log\left(\frac{p(\mathbf{u}(\mathbf{x})|\mathbf{\Theta}_{\mathbf{u},\mathbf{1}})}{p(\mathbf{u}(\mathbf{x})|\mathbf{\Theta}_{\mathbf{u},\mathbf{1}})}\right) - \beta\log\left(\frac{q_1(\mathbf{x})}{q_2(\mathbf{x})}\right)\right]$$

where the weighting parameters α and β have been introduced for the adjustment of the balance between the tensor invariants and tensor orientation terms and to control the effect of the spatial prior, respectively.

III. EXPERIMENTAL RESULTS AND DISCUSSION

The proposed segmentation method is validated by means of two test DTI volumes (hereafter, volumes 1 and 2) [1].

Suitable parameters for the segmentation of the different structures of interest were tuned for DTI volume 1 and this set of parameters was then employed —unless otherwise stated— for the segmentation of DTI volume 2. Table I shows the selected parameters for the different white matter structures.

First, and in order to show the capabilities of the proposed segmentation method, we show in Figure 4 the segmenting surfaces corresponding to different important anatomical structures in the white matter of DTI volume 2. Results for the corpus callosum, cingulum, corona radiata and inferior longitudinal fasciculii show that these anatomical structures are nicely segmented.

[1]Diffusion-weighted images were acquired on a 3T scanner (General Electric Company, Milwaukee, WI, USA) using an echo planar imaging (EPI) sequence, with a double echo option to reduce eddy-current related distortions. To reduce the impact of EPI spatial distortion, an 8 Channel coil and ASSET with a SENSE-factor of 2 were used. The acquisition consisted in 51 directions with $b = 900$ s/mm2, and 8 baseline images with $b = 0$ s/mm2. The scan parameters were: TR = 17 ms, TE = 78 ms, FOV = 24 cm, 144 × 144 encoding steps, 1.7 mm slice thickness. A total of 85 axial slices covering the whole brain were acquired.

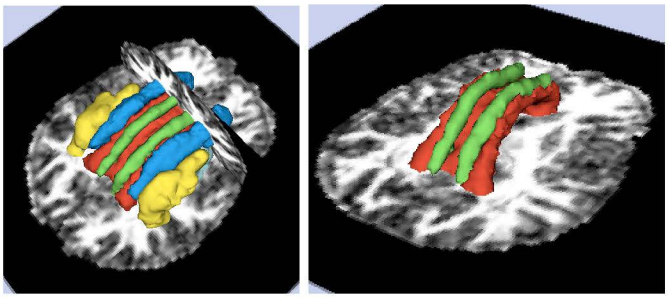

Fig. 4. (Left) Segmentation results for different structures from the DTI volume 2. Segmented structures are corpus callosum (red), cingulum (green), corona radiata (blue), longitudinal fasciculii (yellow) and external capsule (light blue). (Right) Results for the corpus callosum and the cingulum only, from a different viewpoint.

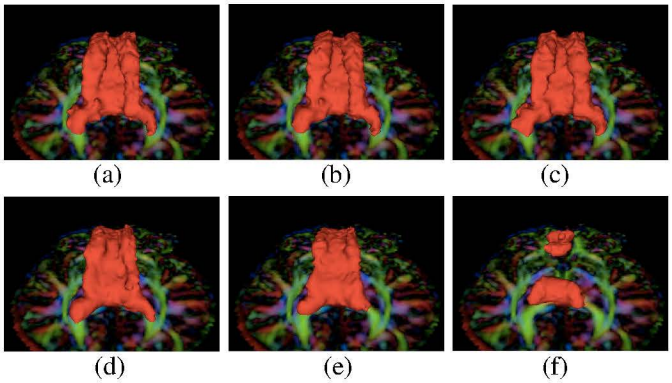

Fig. 5. Segmentation results for the corpus callosum in the test DTI volume using (a) $\alpha = 1$; (b) $\alpha = 0.8$; (c) $\alpha = 0.6$; (d) $\alpha = 0.4$; (e) $\alpha = 0.2$; (f) $\alpha = 0$.

Orientation information is of high relevance for segmentation in DTI. One of the key advantages of the proposed segmentation method is the capability to weigh the importance of the tensor orientation relative to the tensor shape. Recent approaches that rely on the use of intrinsic tensor distances, where the relative importance of the different tensor attributes in the segmentation cannot be controlled, find problems in the segmentation when structures with similar tensor properties are adjacent. Such a situation takes place when segmenting the corpus callosum, because the cingulum, an adjacent structure, is represented by tensors similar in shape but very different in orientation. Figure 5 shows the segmentation results for the corpus callosum in DTI volume 2 for different values of the parameters α and β. When the shape is privileged over the orientation, two parallel ridges appear along the corpus that correspond to parts of the cingulum that are erroneously segmented as belonging to the corpus callosum. When no invariants are considered at all ($\alpha = 0$), however, the orientation by itself is too restrictive and cannot capture the variability of the whole corpus callosum, and therefore the segmentation also fails.

In order to illustrate the importance of the joint use of the spatial prior and the tensor invariants and orientation as tensor features, we show in Figure 6 a comparison between the segmentation of the corpus callosum with and without

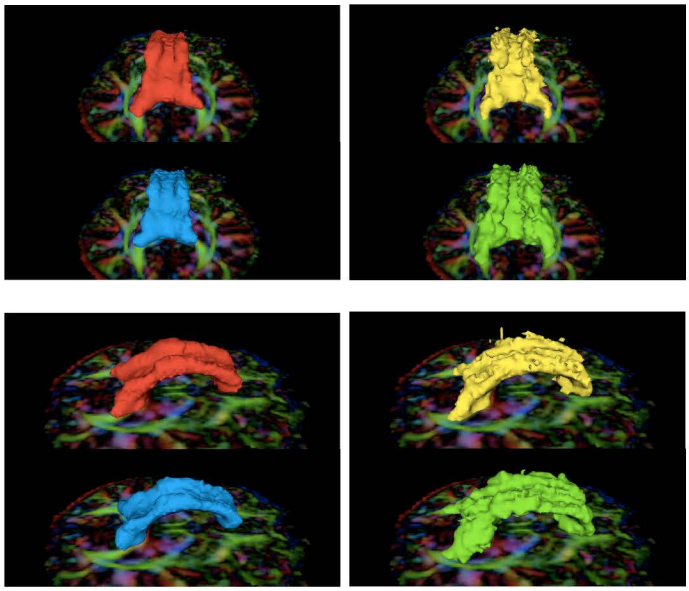

Fig. 6. Comparison of the segmentation of the corpus callosum with the proposed method (red, tensor invariants + orientation and spatial prior), a geodesic tensor distance with spatial prior (yellow), tensor invariants + orientation without spatial prior (blue) and no spatial prior with geodesic tensor distance (green). The geodesic tensor distance has trouble distinguishing between the corpus and the cingulum, as they have similar tensor properties except from the tensor orientation. With no spatial prior, the distal regions of the corpus are not properly extracted.

the spatial prior and using the invariants and orientation or a traditional tensor distance (geodesic distance was employed). It is worth noting that the results, when no spatial prior is used and geodesic distance is applied, correspond to the segmentation method presented in [10].

IV. Conclusions

We have proposed in this paper a novel technique for the segmentation of tensor fields applied to the extraction of anatomical structures from the brain white matter; the method is based on an atlas-registered presegmentation that serves as a prior in the overall optimization procedure. Additionally, tensor invariants and tensor orientation are separately used, so that both terms can be weighted differently according to the properties of the region to be segmented.

We have found that the weighted combination of the three pieces of information indicated above (prior, tensor invariants and tensor orientation) draws better results than other methods reported in the literature and based on intrinsic tensor distances.

V. Acknowledgements

The authors acknowledge the Ministerio de Ciencia e Innovación of Spain for research grant TEC2010-17982, the Fondo de Investigaciones Sanitarias for grant PI11-01492 and the Consejería de Sanidad de Castilla y León for grant SAN103/VA40/11.

References

[1] V. Arsigny, P. Fillard, X. Pennec, and N. Ayache. Log-Euclidean metrics for fast and simple calculus on diffusion tensors. *Magnetic Resonance in Medicine*, 56(2):411–421, 2006.

[2] S. P. Awate, H. Zhang, and J. C. Gee. A fuzzy, nonparametric segmentation framework for DTI and MRI analysis: with applications to DTI-tract extraction. *IEEE Transactions on Medical Imaging*, 16(1):1525–1536, 2007.

[3] P. L. Bazin, C. Ye, J. A. Bogovic, N. Shiee, D. S. Reich, J. L. Prince, and D. L. Pham. Direct segmentation of the major white matter tracts in diffusion tensor images. *Neuroimage*, 58:458–468, 2011.

[4] R. de Luis-Garcia, C.-F. Westin, and C. Alberola-Lopez. Gaussian mixtures on tensor fields for segmentation: Applications to medical imaging. *Computerized Medical Imaging and Graphics*, 35(1):16–30, 2011.

[5] A. Dempster, N. Laird, and D. Rubin. Maximum likelihood from incomplete data via the EM algorithm. *Journal of the Royal Statistical Society*, 39(1):1–38, 1977.

[6] D. B. Ennis and G. Kindlmann. Orthogonal tensor invariants and the analysis of diffusion tensor magnetic resonance images. *Magnetic Resonance in Medicine*, 55(1-2):136–146, 2006.

[7] M. Jenkinson and S.M. Smith. A global optimisation method for robust affine registration of brain images. *Medical Image Analysis*, 5(2):143–156, 2001.

[8] M. Kubicki, R. McCarley, C. Westin, H. Park, S. Maier, R. Kikinis, F. Jolesz, and M. E. Shenton. A review of diffusion tensor imaging studies in schizophrenia. *Journal of Psychiatric Research*, 41(1-2):15–30, 2007.

[9] C. Lenglet, M. Rousson, and R. Deriche. Segmentation of 3d probability density fields by surface evolution: Application to diffusion mri. In *Proc. of the Conference on Medical Image Computing and Computer Assisted Intervention (MICCAI)*, Saint Malo, France, sep. 2004.

[10] C. Lenglet, M. Rousson, and R. Deriche. DTI segmentation by statistical surface evolution. *IEEE Transactions on Medical Imaging*, 25(6):685–700, 2006.

[11] S. Mori, S. Wakana, P.C.M. van Zijl, and L.M. Nagae-Poetscher. *MRI Atlas of Human White Matter*. Elsevier Science, 1st edition, 2005.

[12] E. Muñoz-Moreno, R. Cardenes-Almeida, and M. Martin-Fernandez. *Review of Techniques for Registration of Diffusion Tensor Imaging*, pages 273–297. Springer London, 2009.

[13] N. Paragios and R. Deriche. Geodesic active regions: A new framework to deal with frame partition problems in computer vision. *Journal of Visual Communication and Image Representation*, 13:249–268, 2002.

[14] P.R. Rodrigues, A. Jalba, P. Fillard, A. Vilanova, and B.M. ter Haar Romeny. A multi-resolution watershed-based approach for the segmentation of diffusion tensor images. In *MICCAI Workshop on Diffusion Modelling*, pages 161–172, 2009.

[15] J. Ruiz-Alzola, C.-F. Westin, S. K. Warfield, C. Alberola, S. Maier, and R. Kikinis. Nonrigid registration of 3D tensor medical data. *Medical Image Analysis*, 6(2):143–162, 2002.

[16] T. M. Salmenpera, R. J. Simister, P. Bartlett, M. R. Symms, P. A. Boulby, S. L. Free, G. J. Barker, and J. S. Duncan. High-resolution diffusion tensor imaging of the hippocampus in temporal lobe epilepsy. *Epilepsy Research*, 71:102–106, 2006.

[17] C. E. Sexton, U. G. Kalu, N. Filippini, C. E. Mackay, and K. P. Ebmeier. A meta-analysis of diffusion tensor imaging in mild cognitive impairment and alzheimers disease. *Neurobiology of Aging*, 32:2322.e5–2322.e18, 2011.

[18] S.M. Smith, M. Jenkinson, M.W. Woolrich, C.F. Beckmann, T.E.J. Behrens, H. Johansen-Berg, P.R. Bannister, I. Drobnjak M. De Luca, D.E. Flitney, R. Niazy, J. Saunders, J. Vickers, Y. Zhang, N. De Stefano, J.M. Brady, and P.M. Matthews. Advances in functional and structural MR image analysis and implementation as FSL. *Neuroimage*, 23(S1):208–219, 2004.

[19] P. C. Sundgren, Q. Dong, D. Gómez-Hassan, S. K. Mukherji, P. Maly, and R. Welsh. Diffusion tensor imaging of the brain: review of clinical applications. *Neuroradiology*, 46(5):339–350, aug. 2004.

[20] S. Wakana, H. Jiang, M. Nagae-Poetscher, P. C. M. van Zijl, and S. Mori. A fiber-tract based atlas of human white matter anatomy. *Radiology*, 230:77–87, 2004.

[21] Z. Wang and B. Vemuri. An affine invariant tensor dissimilarity measure and its applications to tensor-valued image segmentation. In *Proc. of the IEEE Conference on Computer Vision and Pattern Recognition*, pages 228–233, Washington DC, USA, 2004.

[22] Y. T. Weldeselassie and G. Hamarneh. DT-MRI segmentation using graph cuts. In J. P. W. Pluim and J. M. Reinhardt, editors, *Proceedings of Medical Imaging, SPIE*, San Diego, CA, USA, February 2007.